Submitted to the Fifth National Conference on Synchrotron Radiation Instrumentation
Madison, WI, June 21-25, 1987

BNL--41291

COA DE88 010664

The NSLS VUV Undulator: Spectral Characteristics and Operating Experience *

Peter D. Johnson

Physics Department, Brookhaven National Laboratory, Upton, NY 11973,

John Galayda, Steven L. Hulbert, Roger W. Klaffky,
Alfredo Luccio, and Gaetano Vignola

National Synchrotron Light Source, Brookhaven National Laboratory, Upton, NY 11973,

and

Chris Jacobsen

Department of Physics, State University of New York at Stony Brook,
Stony Brook, New York 11794

Abstract

The design and operating characteristics of the VUV undulator installed on the NSLS VUV ring are presented. Specifically, the spectral output through three circular on-axis pinholes of different diameters has been measured. Near the minimum magnetic gap (40mm), the flux into a 0.25 mrad circular aperture at the peak of the fundamental ($h\nu = 57$ eV) is $\approx 1 \times 10^{14}$ photons/sec/0.1A/1%BW. We find good agreement in spectral shape between these measured spectra and spectra calculated by integrating the theoretical undulator emission spectrum over the relevant spatial variables and including electron beam emittance. We also show calculated zero-emittance and on-axis flux spectra for comparison. A description is given of the beam line and monochromator currently installed on this undulator for the purpose of performing spin-resolved photoemission.

*This work was performed under the auspices of the U.S. Dept. of Energy, under contract no. DE-AC02-76CH00016.

I. Introduction

Undulators and wigglers currently are being installed on a number of existing storage rings and are planned as the primary source of photons on other storage rings now in the design phase. In this paper we present results from the initial operation of a VUV undulator installed on the NSLS VUV ring at Brookhaven. In particular, we present results obtained from a beam line designed for spectroscopy experiments and constructed to exploit the VUV radiation emitted from the undulator central to the former Free Electron Laser (FEL) project at the NSLS. The original small gap (≥20mm) undulator for this experiment [1-4] has been recommissioned as an "out-of-vacuum" device operating in the VUV photon energy range. The magnetic gap can be varied from 39mm to infinity, which produces fundamental radiation from 53eV to 81eV. Insertion devices operating at other institutions with fundamental radiation in this photon energy range include beam line BL3A1 at the 750 MeV storage ring UVSOR in Okazaki (Japan) [5] and the multipole wiggler on the 5.3 GeV storage ring DORIS II in Hamburg (FRG) [6,7]. Undulators at BESSY in Berlin (FRG), Super ACO in Orsay (France), Aladdin in Stoughton, Wisconsin (USA), and SSRL in Stanford, California (USA) will also operate with fundamentals in the VUV/soft x-ray photon energy range.

We present the design and operating characteristics of the NSLS VUV undulator near its minimum magnetic gap. We find that the spectral shape of the total flux output (photons/sec/100mA ring current/1% bandwidth) from this device, measured through on-axis circular pinholes of varying sizes, agrees well with spectra calculated by integrating theoretical undulator emission over the relevant spatial variables and including electron beam emittance. However, the measured and calculated intensities differ. The calculations provide added insight into undulator radiation patterns by demonstrating their dependence on physical variables such as electron beam size and electron beam angular spread.

We are using this undulator as an intense source of photons for a program based on spin-polarized photoemission. In Section II, we recall the basic equations which govern the undulator spectral output and describe the physical characteristics of the undulator, including the results of magnetic measurements and operational effects on the NSLS VUV ring; in Section III we present the measured undulator output flux spectra; in Section IV we present the calculated spectra and their dependence on various physical variables; and in Section V we present our conclusions.

II. The NSLS VUV Undulator (U5U)

The output characteristics of undulators have been described in detail elsewhere. Briefly, the spectral output consists of a series of harmonics whose wavelength λ_n is given by

$$\lambda_n(K,\theta)=\frac{\lambda_u}{2n\gamma^2}\left(1+\frac{K^2}{2}+\gamma^2\theta^2\right), n=1,3,5,\ldots \quad (1)$$

where $\gamma = 1456$ is the storage ring energy (744 MeV) in electron rest mass units, λ_u is the magnetic period length, θ is the observation angle with respect to the undulator axis, and

$$K = \frac{e}{2\pi mc} B_0 \lambda_u = 0.934 B_0(T) \lambda_u (cm) \qquad (2)$$

is the standard magnetic strength parameter related to B_0, the peak magnetic field strength. For $K \approx 1$ (the so-called undulator regime), the angular deflection of the electron beam in the device $(\frac{K}{\gamma})$ is comparable to the maximum angular deflection of the emitted light and the spectral output is dominated by characteristic harmonic peaks (see Fig. 1). As θ is increased from zero, the odd harmonic peaks broaden on the low energy (long wavelength) side and the even harmonics begin to appear.

The natural bandwidth broadening of the odd harmonics is given approximately by

$$\frac{\Delta\lambda}{\lambda} \approx \frac{1}{nN} \qquad (3)$$

and the rms opening angle of emission from the odd harmonics is

$$\sigma_{r'} \approx \frac{1}{\gamma}\left(\frac{1+\frac{K^2}{2}}{2nN}\right)^{1/2} = \left(\frac{\lambda}{L}\right)^{1/2}. \qquad (4)$$

where $L = N\lambda_u$ is the total length of the undulator.

It is essential to note that equations (1), (3), and (4) apply only for a zero-emittance electron beam: to the extent that the electron beam angular spread $\sigma_{x'}, \sigma_{y'}$ is a significant fraction of the natural emission angle $\sigma_{r'}$, all of the above formulae are modified in a non-simple way. Crudely speaking, if the electron beam angular divergence or the range of observation angles is large compared to the $\sigma_{r'}$ ($\sigma_{r'} \approx 100\mu rad$ for the U5U undulator), equation (1) applies to the even harmonics as well. The more exact approach involves numerical integration over the relevant physical variables. The calculated flux output of the NSLS VUV undulator is presented in Section IV along with its dependence on physical variables such as the electron beam vertical angular divergence.

As noted in the introduction, the U5U undulator was originally designed for a FEL project and subsequent modifications allow it to operate as an "out-of-vacuum" device, i.e. the magnets are now located outside the vacuum vessel of the storage ring. The structure of this permanent magnet undulator is of the classical "Halbach" type, with eight $SmCo_5$ blocks per magnetic period (four above and four below the median plane), and a total number of periods N = 38. The magnetic period length λ_u = 6.5cm, the horizontal width of the blocks (perpendicular to the magnetic axis in the orbital plane) is 5.0 cm, and the minimum vertical gap 2g is 39mm, principally determined by the outside thickness of the storage ring vacuum vessel and the position of the fringe field correction magnets.

While the undulator was removed from the storage ring for "out-of-vacuum" conversion, the four $SmCo_5$ blocks at the extreme ends of the device were removed and reduced in dimension along the beam path from 1/4 period to 1/8 period, halving their dipole moments. These four blocks must be positioned to cancel the net dipole field integral in the rest of the undulator, which is equivalent to the effect of only two 1/4-period blocks. Originally, the contribution of the four end blocks was cut in half not by cutting the blocks in half but by moving them away from the beam axis and rotating them by 20°. This arrangement did not simultaneously cancel the sextupole field integral of the undulator. If one assumes that the magnet blocks have fixed magnetizations, so that their fields can be superposed, it follows that blocks with 1/2 strength will, in principle, cancel all integrated multipoles for all gap settings [8]. In practice, the re-mounted end correction blocks reduced the sextupole field integral by a factor of four, to less than 1 Tesla/meter. The dipole field integral was reduced to 10^{-4} *Tesla·meter*. At a gap of 39mm, the vertical tune shift caused by the undulator is $\Delta\nu_y = 0.005$. The steering magnets and quadrupoles nearest the undulator are adjusted to localize and minimize the effect of the undulator on the electron optics.

III. Measured flux output

The experimental spectra shown in this paper were all measured on a spectroscopy beam line that has been described in detail elsewhere [9]. Briefly, light from the undulator is deflected by a plane mirror onto a paraboloid, which then focuses it onto the entrance slit of a miniature toroidal grating monochromator (TGM). This monochromator, the so-called Cricket TGM, was originally designed for use with a He discharge lamp source. Featuring a small one-meter radius 1200 line/mm grating, a 22cm entrance arm, and a 30 cm exit arm, it is physically well matched to the narrow undulator emission. Operated in first inside order with an included angle of 150 degrees, it covers the photon energy range from 25eV to 150eV with reasonable resolution. For example, at the peak of the fundamental near minimum gap ($h\nu = 57$eV) the source size limit for 10μm slits is 21meV [9]. Apertures of different diameters can be inserted into the beam line upstream of the first mirror in order to allow measurements of the output from the undulator as a function of angular divergence.

The spectral output of the undulator is obtained from the measured photon flux using the following correction procedure, which attempts to take into account all of the transmission losses introduced by the collection and focusing mirrors and the monochromator: second order contamination is crudely removed by subtracting a small fraction of the spectrum at $2\times h\nu$ from the spectrum at $h\nu$. The electron yield from the sample is converted to photons/sec incident upon the sample via the photon-energy dependent quantum efficiency and the soft x-ray reflectivity of the sample. The sample-to-ground current at the peak of the fundamental (with 35μm monochromator slits and 209mA in the VUV ring) is 32nA. The resulting spectral output must be corrected for the photon-energy dependence of the monochromator bandwidth and scaled to 0.1A ring current. Finally, the resulting spectrum must be corrected for the transmission losses of the entrance slit, the reflectivity losses of the collecting and focusing mirrors, and the overall efficiency of the grating in first order. We estimate that the errors of omission or incorrect estimation in this corrected undulator spectrum amount to possibly a factor of two.

With a magnetic gap 2g = 40mm and K = 0.92 (B_0 = 0.15T), the measured spectral output (photons/sec/0.1A ring current/1% bandwidth) of the NSLS VUV undulator (U5U) through a 2mm diameter on-axis circular pinhole at a distance D = 8m from the center of the undulator is shown in Fig. 1. The first ($h\nu = 57$eV) and second ($h\nu = 111$eV) harmonics of the undulator output lie within the photon energy range covered by our monochromator. Note the rather large dynamic range of the measured undulator output: the harmonic peaks are two orders of magnitude stronger than the relatively flat true background upon which they sit. Spectra taken with the stored beam energy reduced from 744MeV to 670MeV show the proper γ-dependence of the undulator output as predicted by equation (1), with the fundamental photon energy shifting to 46eV at $K = 0.92$.

The spectral output of the undulator in the first harmonic as a function of on-axis pinhole size is shown in Fig. 2. The spectral broadening of the low energy side of the fundamental with increasing pinhole size agrees quantitatively with that of emission spectra calculated by the method described in Sect. IV. In addition, 2mm pinhole spectra taken as a function of vertical and horizontal displacement relative to the undulator axis show the correct dependence on observation angle θ as described by equation (1).

IV. Calculated flux output

The method used for obtaining the calculated undulator spectra shown has been described elsewhere [10]. Briefly, it involves integrating the expression for spectral output of an ideal undulator [11-15] over a weighted function combining both the electron beam size and divergence at a specified distance from the undulator. The technique has the advantage that while the number of integration variables involved is reduced, allowing for efficient computation, it calculates the full, emittance-included intensity at an observation point or within an observation aperture located on or off the undulator axis. The result of such a calculation for a 2mm diameter on-axis pinhole at $D = 8m$ is shown as a solid line in Fig. 1. The electron beam parameters in the U5U straight section of the NSLS VUV ring used for this calculation were $\sigma_x = 1200\mu m$, $\sigma_{x'} = 88\mu rad$, $\sigma_y = 70\mu m$, and $\sigma_{y'} = 13\mu rad$ For comparison, the corresponding zero-emittance spectrum (angle-integrated over a 2mm diameter circular aperture at $D = 8m$) is shown in Fig. 1 as a dot-dashed line, and the on-axis spectrum (including electron beam emittance) scaled to the angle accepted by a 2mm diameter circular aperture at $D = 8m$ is shown in Fig. 1 as a dotted line. Note that because of the effect of the emittance of the NSLS VUV ring on this undulator, the flux into a 2mm circular aperture at $D = 8m$ contains strong "contamination" by the even harmonics ($n = 2$ is the only even harmonic shown) and considerable broadening of all harmonics: the intrinsic linewidth $\frac{\Delta\lambda}{\lambda}$ of the first harmonic is approximately 0.3, most of this being caused by the finite electron beam angular divergence ($\frac{\Delta\lambda}{\lambda}$ for a zero emittance electron beam would be 0.1). In contrast, the spectra shown in Fig. 1 are not very sensitive to the vertical electron beam size σ_y, because $\frac{\sigma_y}{D} << \sigma_{y'}$. Tripling σ_y in the calculations decreases the first harmonic intensity by $<1\%$ and increases the second harmonic intensity by $\approx 15\%$ without changing its width.

At the peak of the first (second) harmonic output of the undulator, the measured spectrum is a factor of 10 (5) lower in flux than the calculated spectrum, but the spectral shape agrees well. Apart from the errors of estimation discussed in Sect. III above, the discrepancy in intensity is most likely due to axial magnetic field errors. Although the magnetic gap-to-width ratio $(\frac{2g}{w})$ transverse to the electron beam is larger than desired $(\frac{2g}{w} \geq 0.8)$, this potential degradation of the flux from the undulator probably does not have a significant effect on its spectral output.

As already noted, both the experimentally measured and the calculated spectral output in Fig. 1 show a strong second harmonic component on axis. This effect is not anticipated in the zero-emittance formulation (Eq. 1) and is a reflection of the finite emittance of the stored electron beam. We demonstrate this in Fig. 3 where we show the calculated spatial and spectral characteristics of the first and second harmonic components, both with zero emittance and finite emittance in the electron beam. These intensity contour plots in $(h\nu,\theta)$ space (so-called omega-theta plots) demonstrate many properties of undulator output and provide a comprehensive record of its spatial and spectral dependences. Note the general decrease of peak energy with increasing θ as described by Eq. 1, the absence of the second harmonic component on axis if electron beam emittance is not included, and the strong effects on the shapes of the contours produced by finite electron beam emittance (a small portion of the third harmonic is seen far off axis in Fig. 3d). These plots are very useful for estimating the photon energy dependence of the flux through a particular on-axis or off-axis aperture.

V. Conclusions

Good agreement in spectral shape is found between the calculated and measured output of the NSLS VUV undulator, although the peak intensities disagree by a factor of 5 to 10. We note the observation of strong even harmonics on axis as a result of the finite emittance of the stored electron beam. Thus, the second harmonic should prove to be a useful flux of photons for spectroscopic experiments. However, the observation of a similar spatial dependence for the first and second harmonic components precludes the possibility of baffles or apertures as a means of second harmonic suppression in the beamline.

The enhanced output flux of this undulator compared to a bending magnet on the NSLS VUV ring makes this source ideal for inherently low-efficiency experiments. One such experiment is spin-polarized photoemission, in which the energy, momentum, and spin of photo-emitted electrons from the surface of a clean magnetic sample are measured. The figure of merit (spin separation $\times$ collection efficiency) of all of the types of spin detectors used for spin-polarized spectroscopy does not exceed 1×10^{-4}. [16] The order-of-magnitude increase in flux provided by the NSLS VUV undulator compared to a 10mrad NSLS VUV dipole source transforms this experiment from almost impossible to fairly tractable. We are using a compact low-energy diffuse scattering type of spin detector developed at NBS [16], which mounts on the exit lens of a standard hemispherical electron energy analyzer and allows easy rotation of the analyzer with respect to the incident photon beam. The results to date are extremely encouraging concerning the feasibility of performing spin-polarized photoemission on an undulator on a low-energy storage ring such as the VUV ring at the NSLS.

The authors wish to acknowledge the grating diffraction efficiency calculations of H. Padmore.

References

1. H. Hsieh, S. Krinsky, A. Luccio, C. Pellegrini, and A. van Steenbergen, Nucl. Instrum. Methods *208* , 79 (1983).
2. A. Luccio and S. Krinsky, in *Free Electron Generators of Coherent Radiation*. Physics of Quantum Electronics, S. F. Jacobs and G. T. Moore, eds., (Addison-Wesley, Reading, MA, 1982), vol. 8, p.181.
3. A. Luccio and L. Yu, in proceedings of the Bendor Free Electron Laser Conference, Bendor, France, Sept.26 - Oct. 1, 1982.
4. Y. Hirai, A. Luccio, and L. Yu, "Study of the Radiation from an Undulator: Near Field Formulation", J. Appl. Phys. *55* , 25 (1984).
5. UVSOR Activity Report UVSOR-13, February, 1986.
6. P. Gurtler, Nucl. Instrum. Methods A *246* , 91 (1986);
7. F. Senf, et. al., Nucl. Instrum. Methods A *246* , 314 (1986);
8. J. Galayda, "Calculation of Field Integrals under a Block of REC". NSLS Technical Note, to be published (1987).
9. P. D. Johnson, S. L. Hulbert, and M. R. Howells, "The Use of a Miniature Toroidal Grating Monochromator on the FEL", BNL Report 37242 (1986).
10. H. Rarback, C. Jacobsen, J. Kirz, and I. McNulty, "The Performance of the NSLS Mini-Undulator", *this volume*; C. Jacobsen and H. Rarback, "Predictions on the Performance of the Soft X-Ray Undulator", in Proceedings of the International Conference on Insertion Devices for Synchrotron Sources, SPIE *582* , 201 (1985); the algorithm discussed in these papers is implemented in the C program entitled "Sensible Modeling of Undulator Throughput", which is available upon request from the authors.
11. D. F. Alferov, Y. A. Bashmakov, and E. G. Bessonov, "Undulator Radiation", Sov. Phys. Tech. Phys. *18* , 1336 (1974).
12. G. K. Green, "Spectra and Optics of Synchrotron Radiation", BNL Report 50522 (1976).
13. S. Krinsky, "An Undulator for the 700 MeV Ring of the National Synchrotron Light Source", Nucl. Instrum. Meth. *172* , 73 (1980).
14. S. Krinsky, "Undulators as Sources of Synchrotron Radiation". IEEE Trans. Nucl. Sci. *NS-30* , 3078 (1983);
15. R. P. Walker, "Spectral Brilliance of Undulators and Wiggler Sources", ESRP Internal Report ESRP-IRM-85/84 (1984).
16. J. Unguris, D. T. Pierce, and R. J. Celotta, Rev. Sci. Intrum. *57* , 1314 (1986).

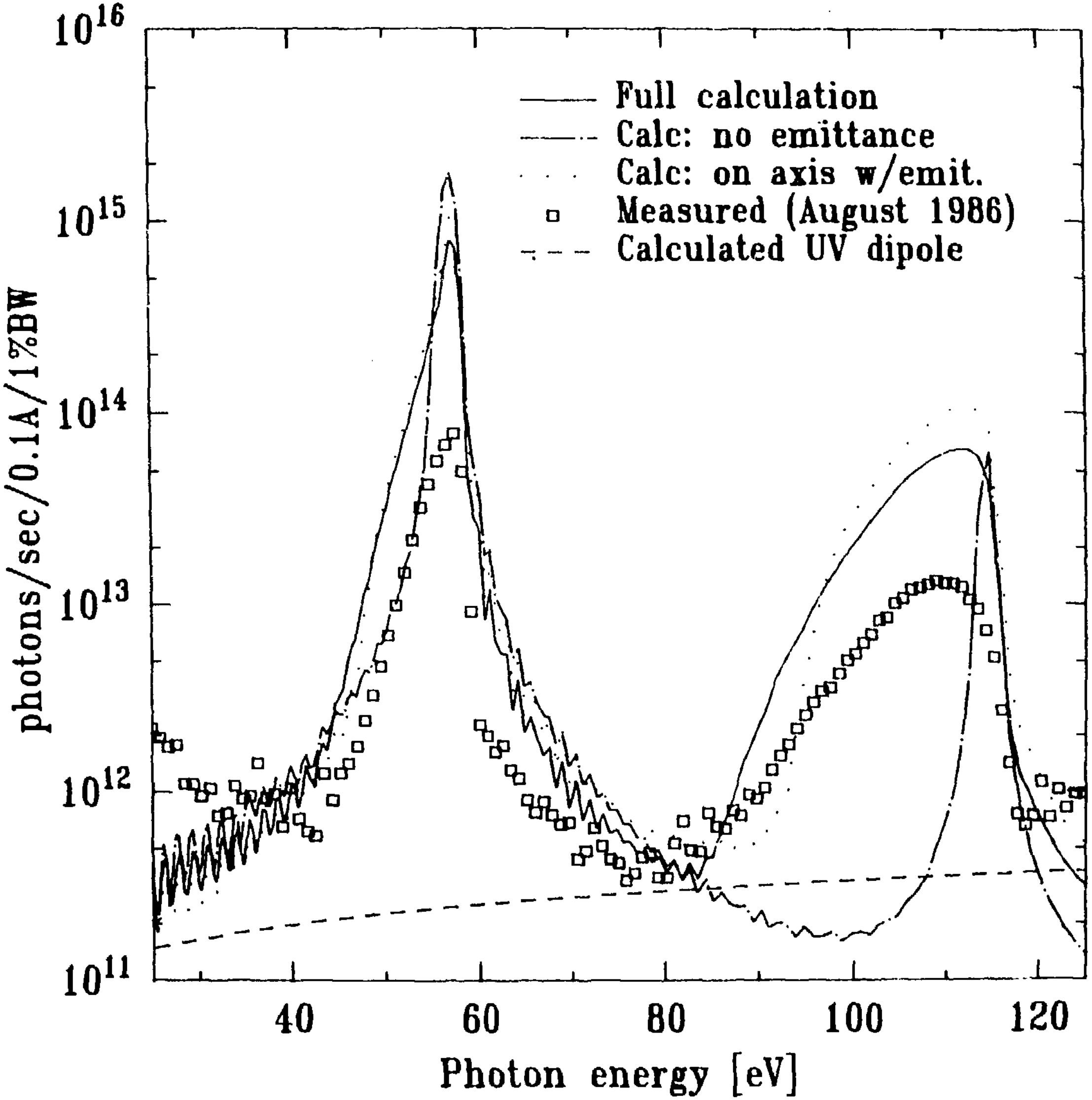

Full calculation
Calc: no emittance
Calc: on axis w/emit.
Measured (August 1986)
Calculated UV dipole
photons/sec/0.1A/1%BW
10^16
10^15
10^14
10^13
10^12
10^11
40
60
80
100
120
Photon energy [eV]

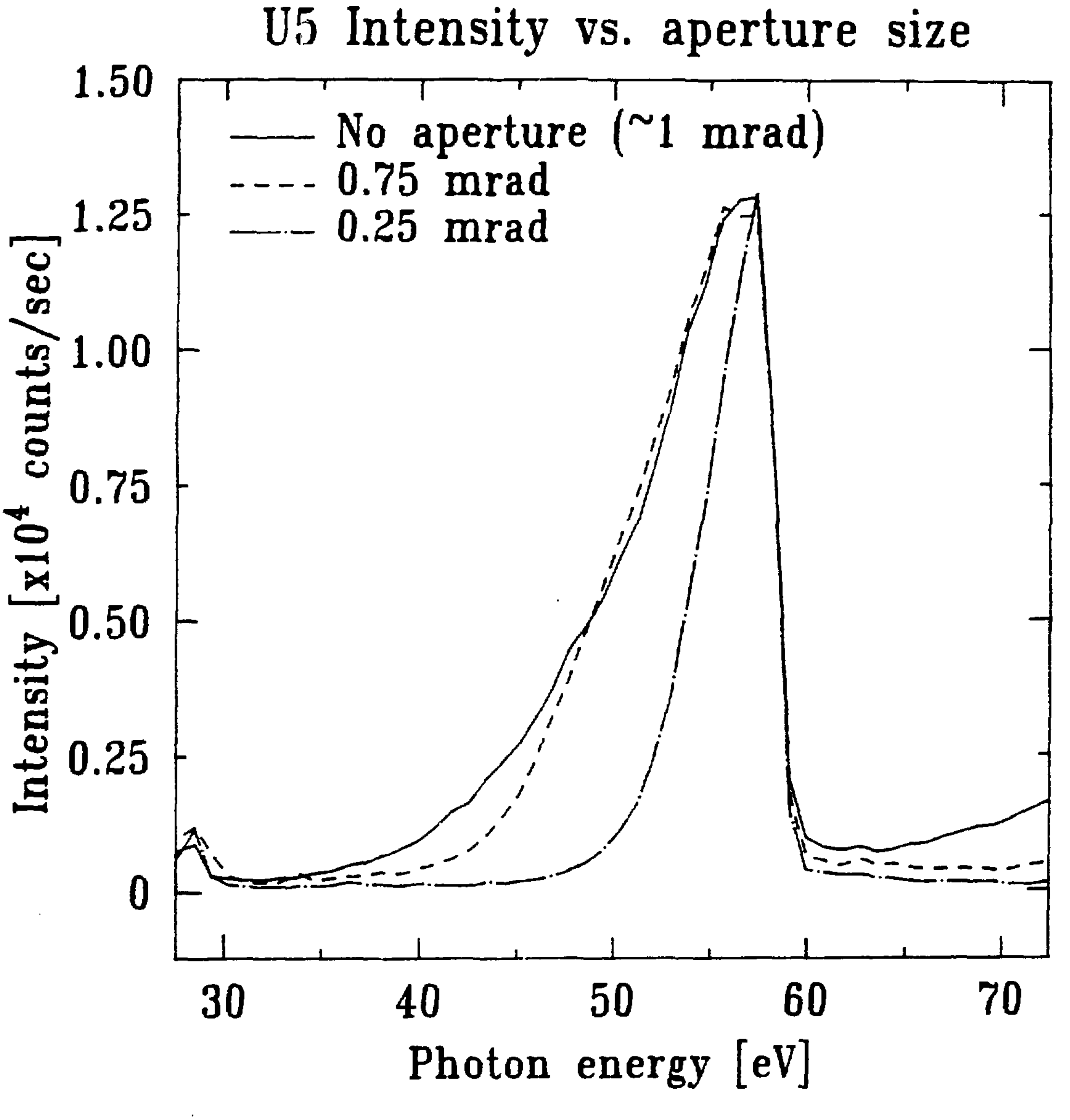

U5 Intensity vs. aperture size
No aperture (~1 mrad)
0.75 mrad
0.25 mrad
1.50
1.25
1.00
0.75
0.50
0.25
0
Intensity [x10^4 counts/sec]
30
40
50
60
70
Photon energy [eV]

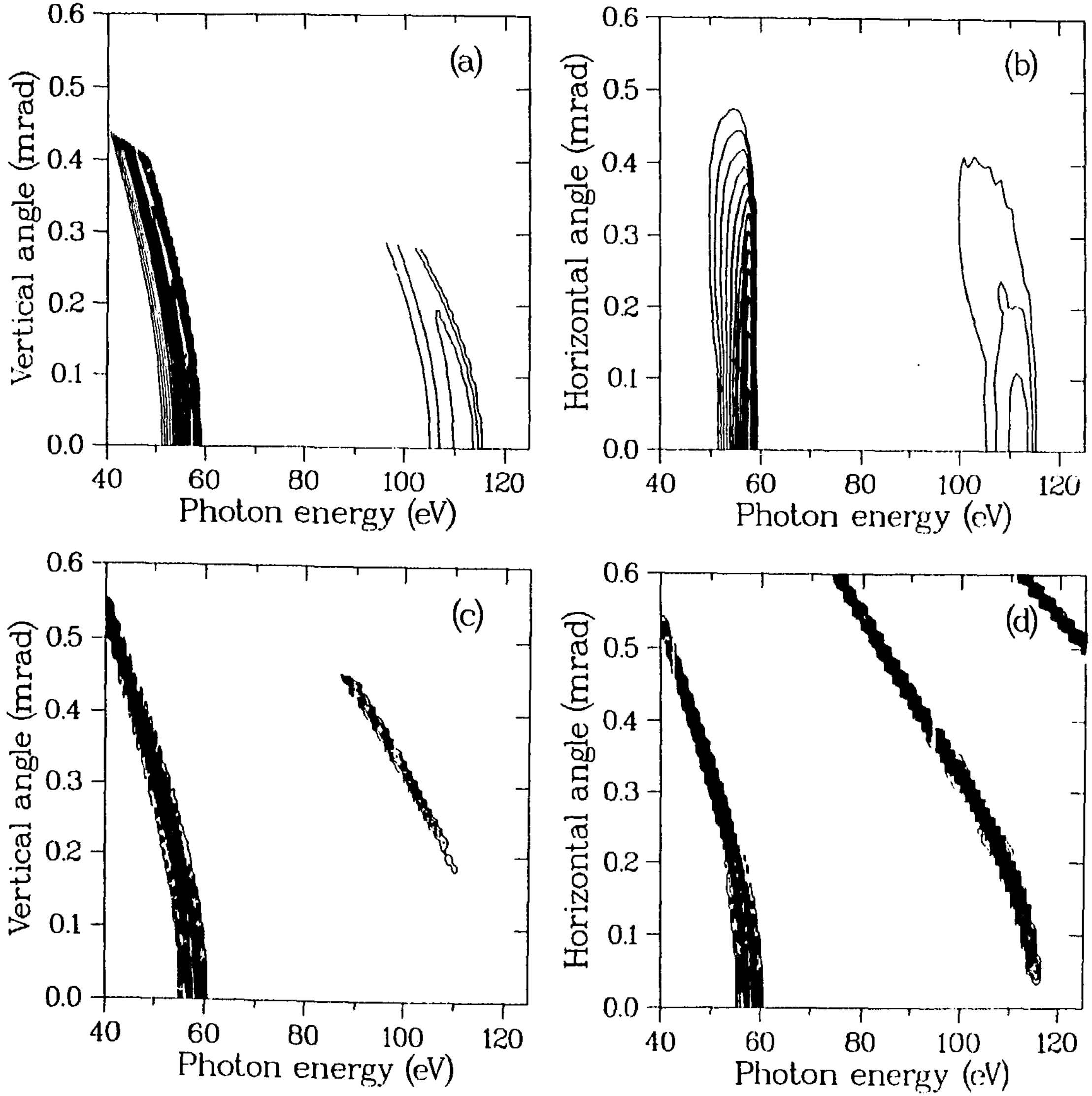
(a)
Vertical angle (mrad)
Photon energy (eV)
(b)
Horizontal angle (mrad)
Photon energy (eV)
(c)
Vertical angle (mrad)
Photon energy (eV)
(d)
Horizontal angle (mrad)
Photon energy (eV)